Edge Electrostatic Fluctuation and Anomalous Transport Characteristics in the Sino-United Spherical Tokamak (SUNIST)

W H Wang

In collaboration with

Y X He, Z Gao, L Zeng, G P Zhang, L F Xie, X Z Yang*, C H Feng*, L Wang*

Department of Engineering Physics, Tsinghua University, Beijing l00084, China

**** Beijing National Laboratory for Condensed Matter Physics，Institute of Physics，Chinese Academy of Sciences, Beijing 100080，China***

outlines

1. Description of experiments
2. Radial distributions of edge plasma parameters
3. Observation of intermittent transport events in SUNIST
4. Summary

1. Description of experiments

Discharge conditions:

$B_T = 0.13$ T;

$I_p = 30$ kA;

loop voltage of 5 V;

2 ms flat-top phase of the plasma current in the ohmic discharges

Diagnostic tools:

- Triple probe to measure electron temperature, density and plasma potential;
- Langmuir probe array to measure the floating potential fluctuations for estimating the radial and poloidal wave numbers;
- Mach probe to measure toroidal plasma flow velocity.

The results reported here are mostly from the triple probe.

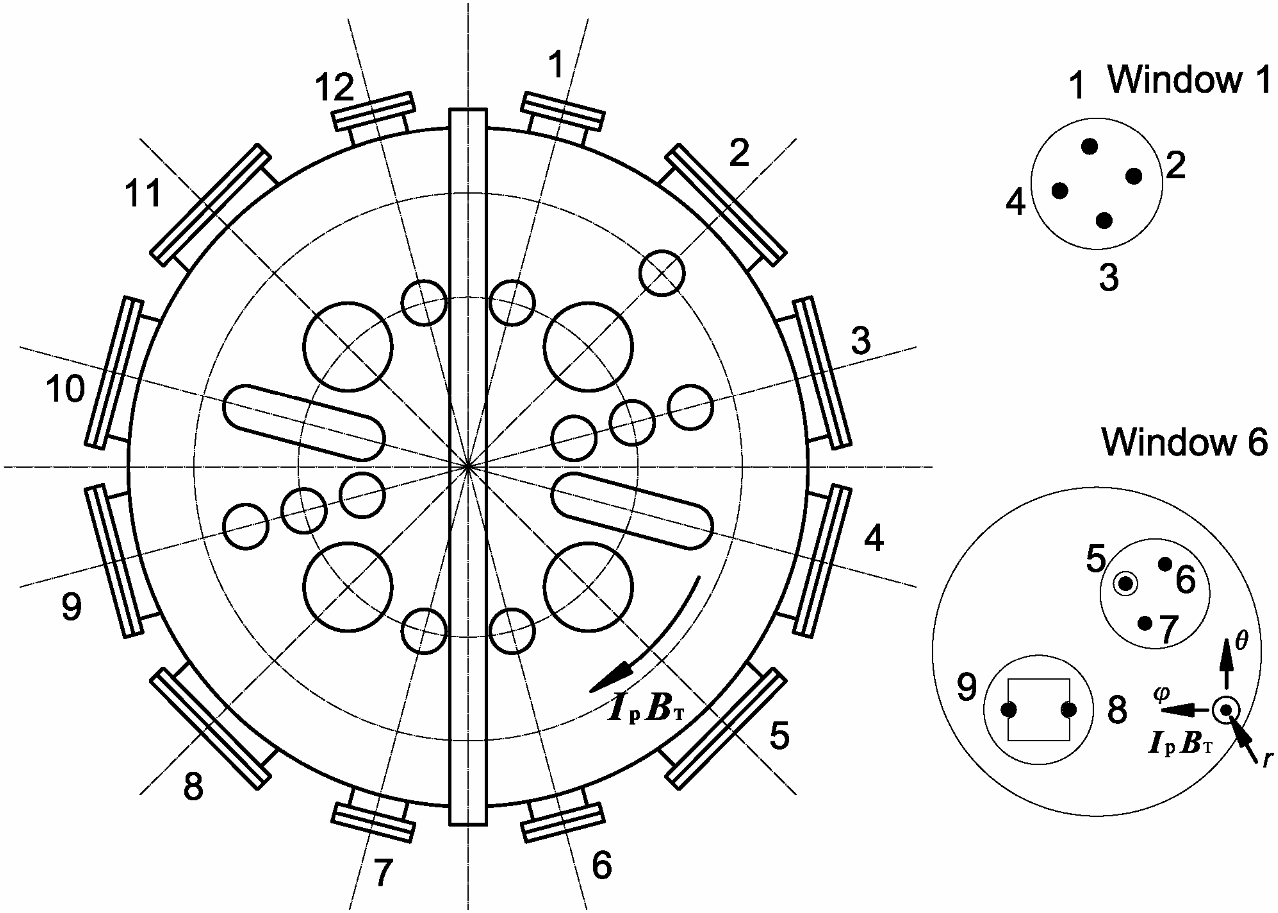

Fig. 1 Relative positions of the windows where the probe arrays are laid, and a closed-up view of the probe structures.

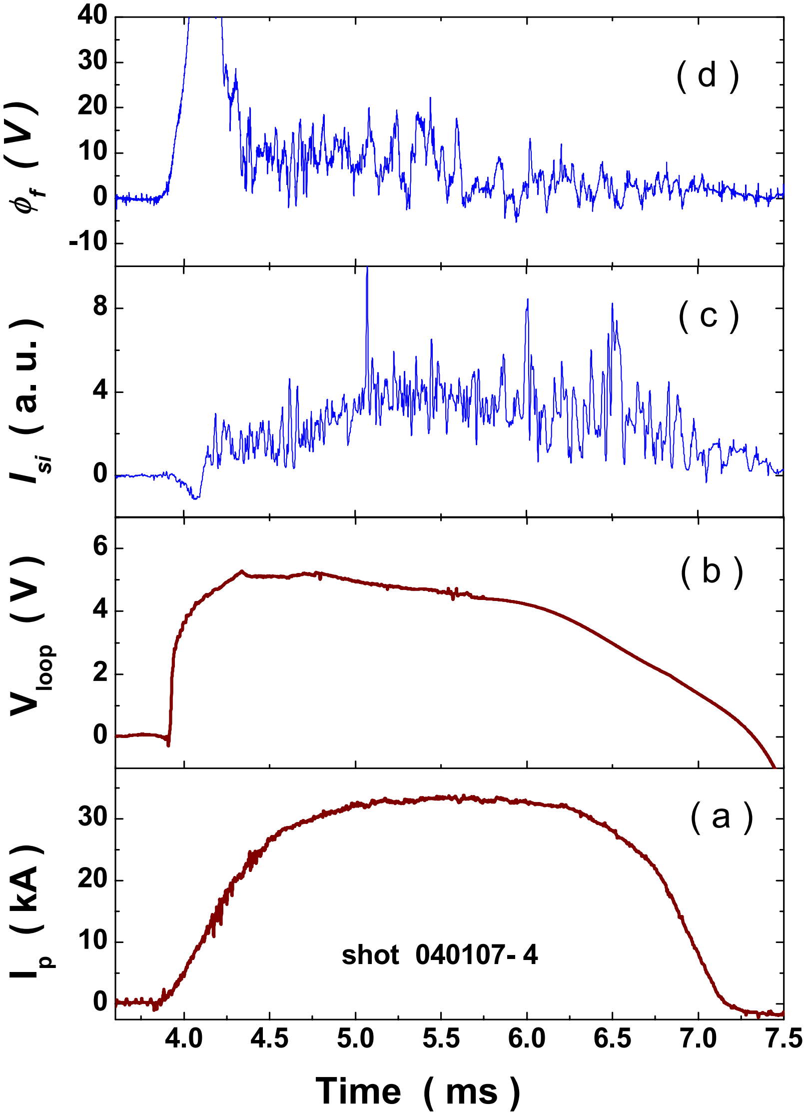

Fig. 2 Typical discharge waveforms of (a) the plasma current, (b) loop voltage, (c) ion saturation current and (d) floating potential.

The data are from the radial position r = 52 cm with probe bias volt –145 V for I_{si} of the triple probe.

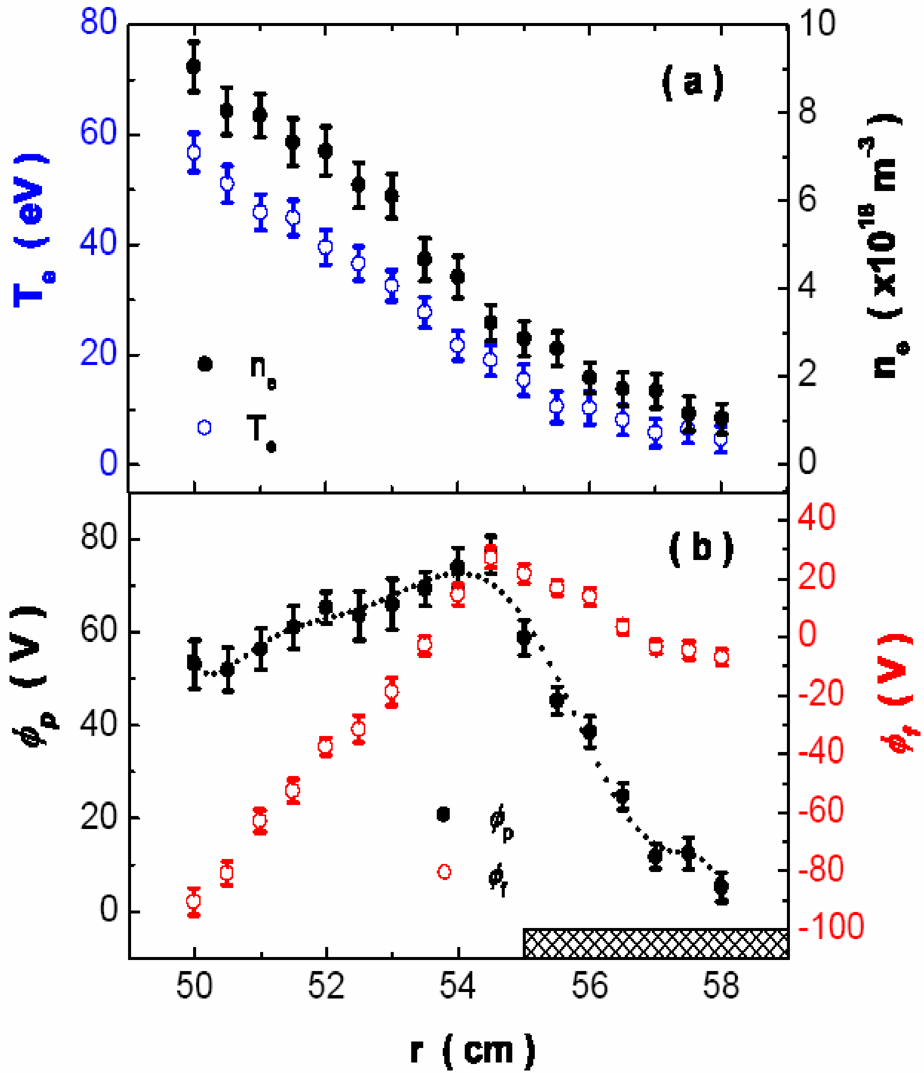

Fig. 3 Radial profiles of equilibrium T_e, n_e, ϕ_f and ϕ_p

Here and hereafter, the error bars are the statistical errors of the ensemble average of 10 ~ 15 shots. The shadow region stands for the radial location of the limiter. The dotted curve in fig 3(b) is the fit curve of the plasma potential.

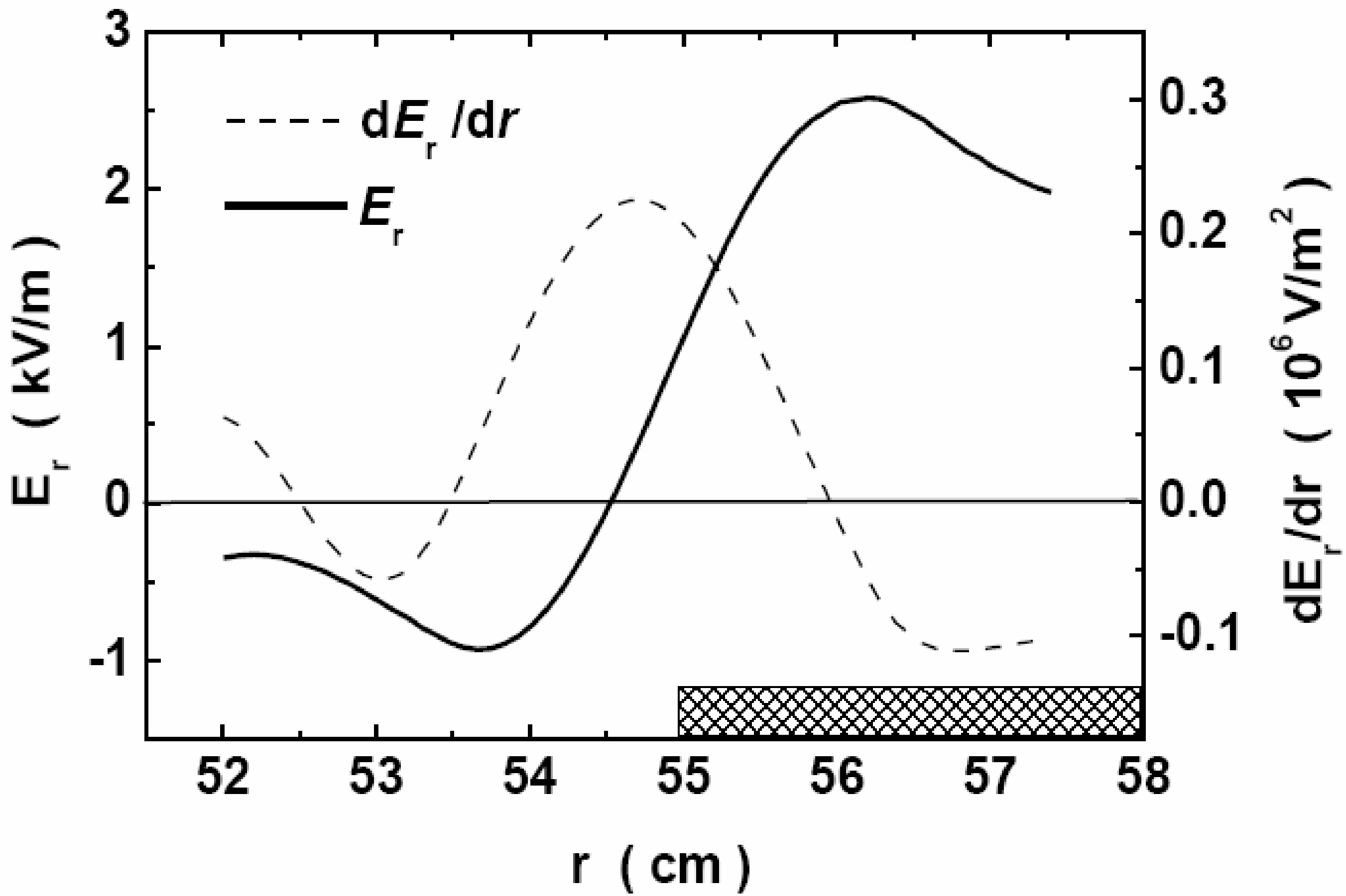

Fig. 4 Radial profiles of radial electric field E_r (estimated from the fit curve of the plasma potential) and its radial gradient dE_r/dr. It can be seen that a naturally formed poloidal velocity shear layer (VSL) is located near the radial position of the limiter.

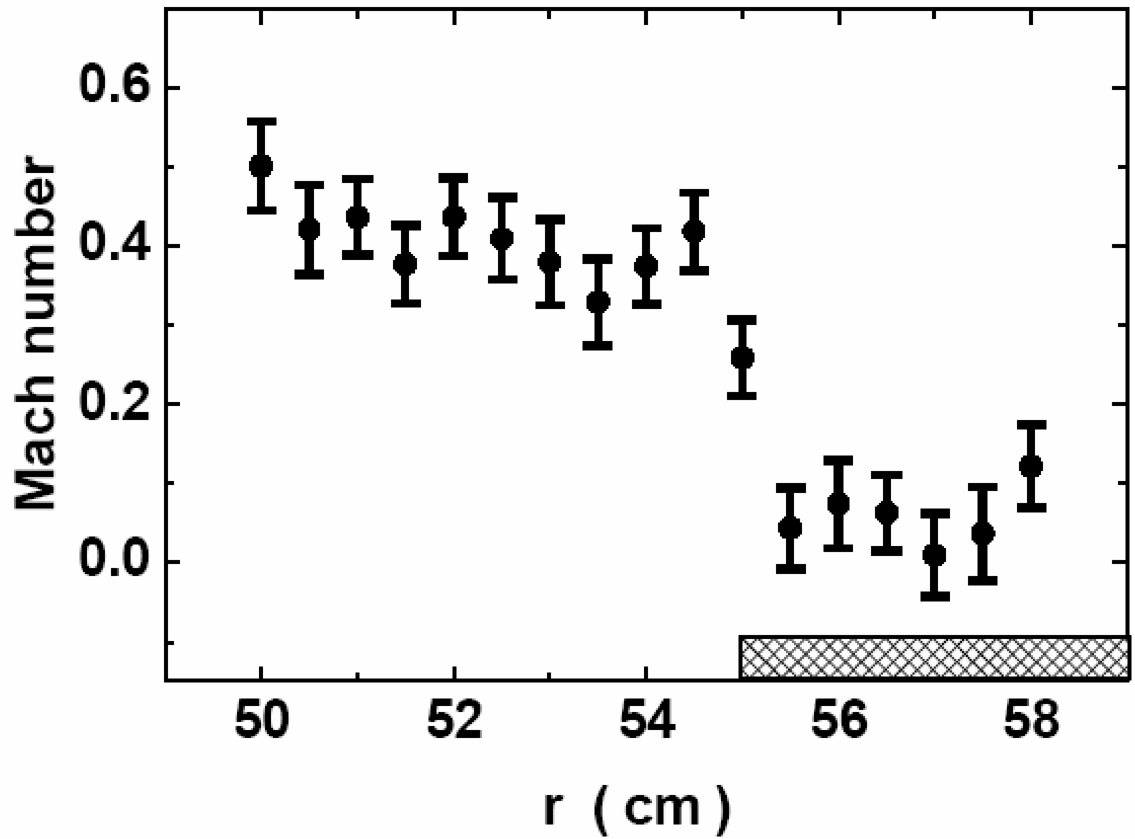

Fig. 5 Radial profile of the toroidal flow velocity Mach number M. In SOL, $M \sim 0.1$ and the toroidal velocity $v_{\phi} \sim 3.4$ km s^{-1}; but in the plasma edge, $M \sim 0.4$ and $v_{\phi} \sim 13$ km s^{-1}. A maximal radial gradient of the v_{ϕ} appears at the radial location of the VSL. Such coincidence was first observed on the TEXT-U tokamak, but it seems not to be reported on the spherical tokamaks so far.

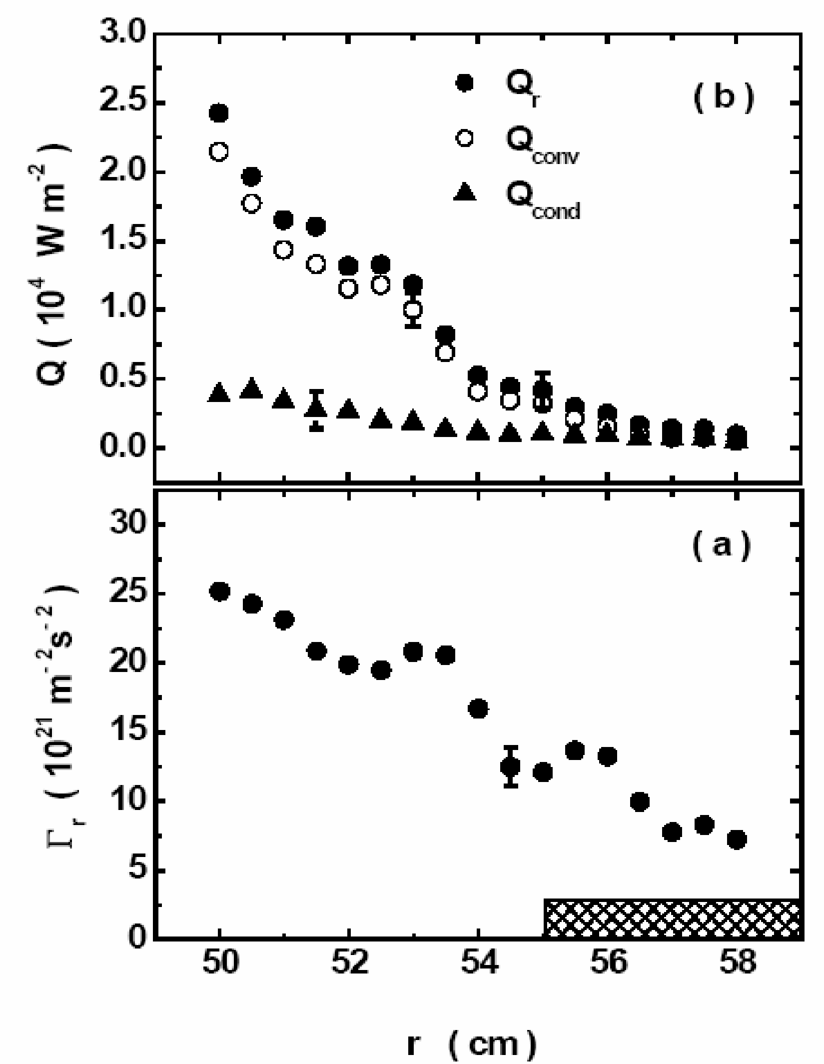

Fig. 6 Radial profiles of (a) the radially turbulence-induced particle fluxes Γ_r, and (b) the heat fluxes Q_r, Q_{conv} and Q_{cond}. Here

$$\Gamma_r = < \tilde{n}_e \tilde{E}_\theta > / B_\phi$$

$$Q_r = Q_{conv} + Q_{cond} = \frac{3}{2} T_e \Gamma_r + \frac{3n_e}{2B_\phi} \left\langle \tilde{T}_e \tilde{E}_\theta \right\rangle$$

$$\tilde{E}_\theta(t) = (\tilde{\phi}_{f3}(t) - \tilde{\phi}_{f1}(t)) / \Delta_\theta$$

It is clear that both fluxes increase with the probe radially moves toward the plasma edge, and the Q_r is mainly contributed by the convective transport item Q_{conv}

3. Observation of intermittent transport events in SUNIST

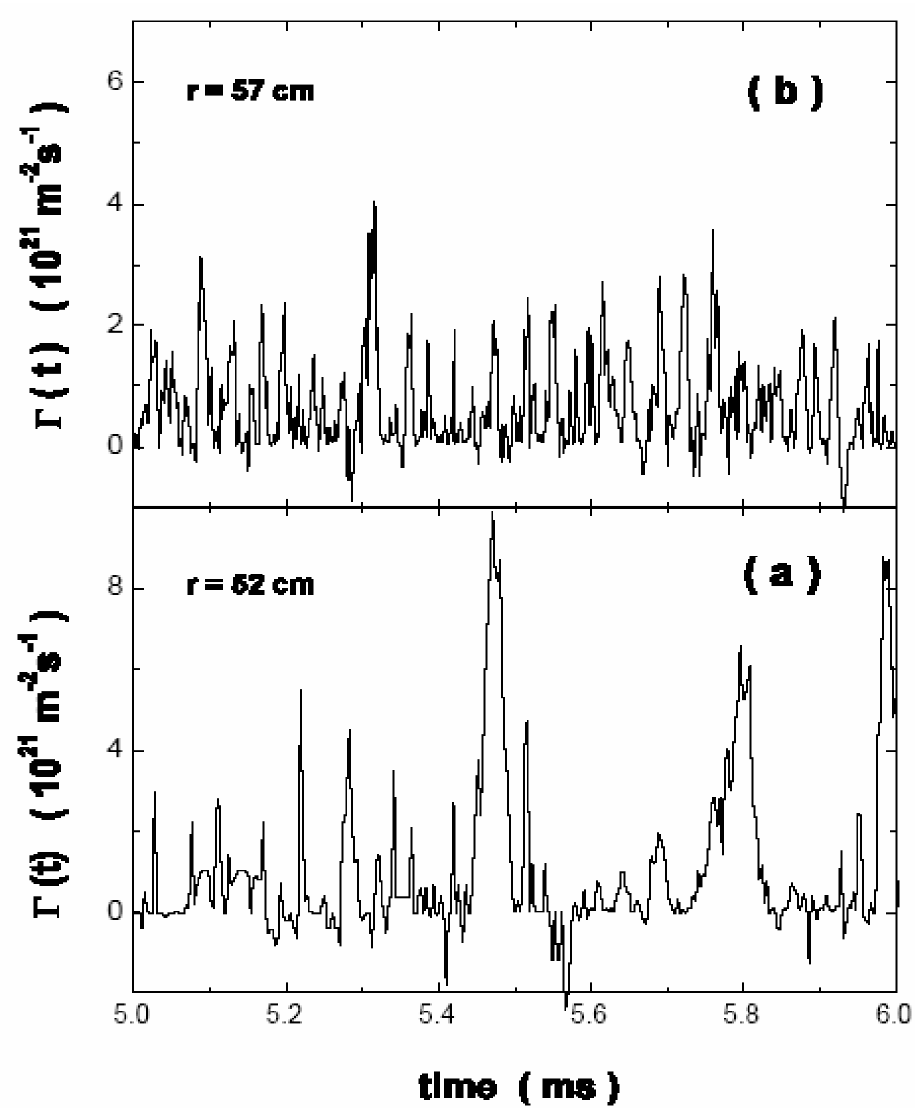

Fig. 7 Comparison of the particle flux patterns between the data from SOL and that from plasma edge.

We can see that both have short-time scale intermittent transport character, but in the plasma edge the transport pattern looks more like "bursty".

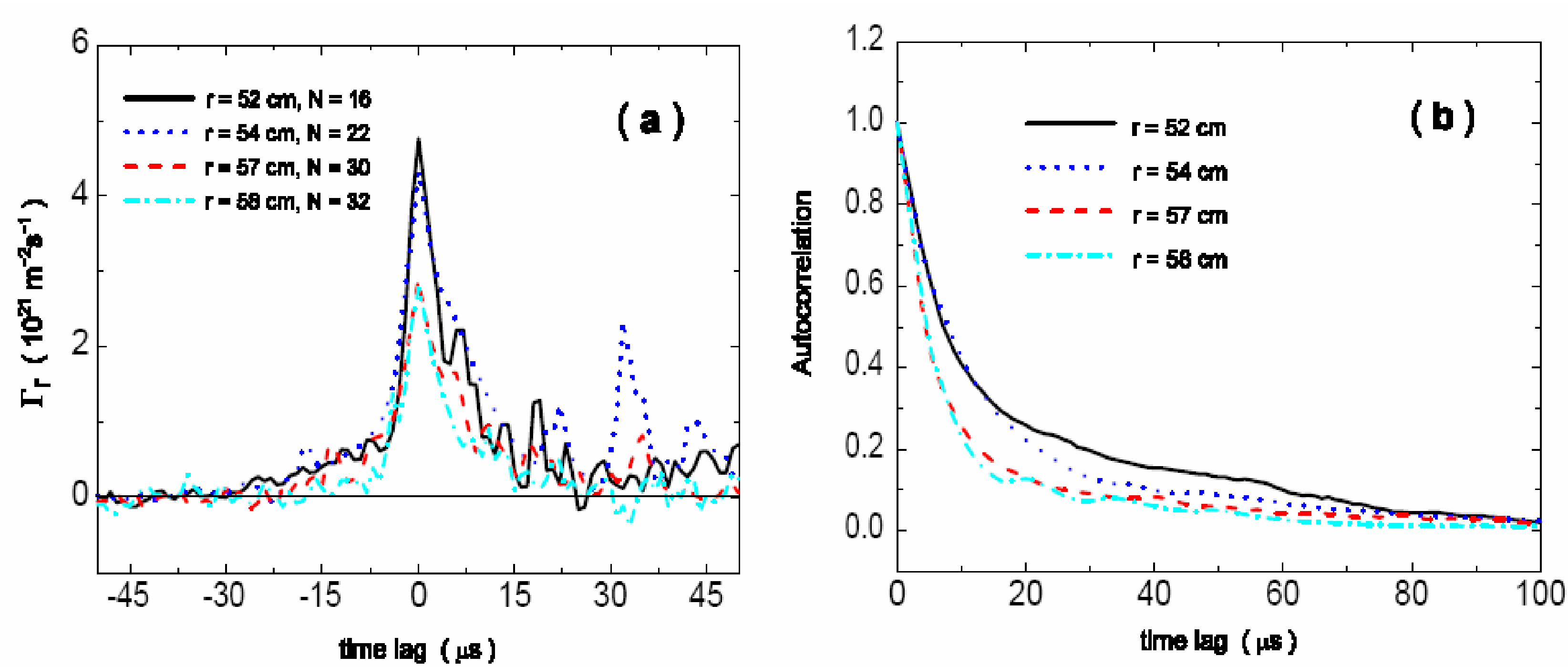

Fig.8 (a) Conditional averaging results (A 2.5×rms-level threshold amplitude is used to discriminate the intermittent events in fluxes) and (b) autocorrelation functions (the positive wings) of the fluxes from four radial positions.

With the density increases, the large events develop faster than that in low density case, despite the number of them decreasing to half of the former.

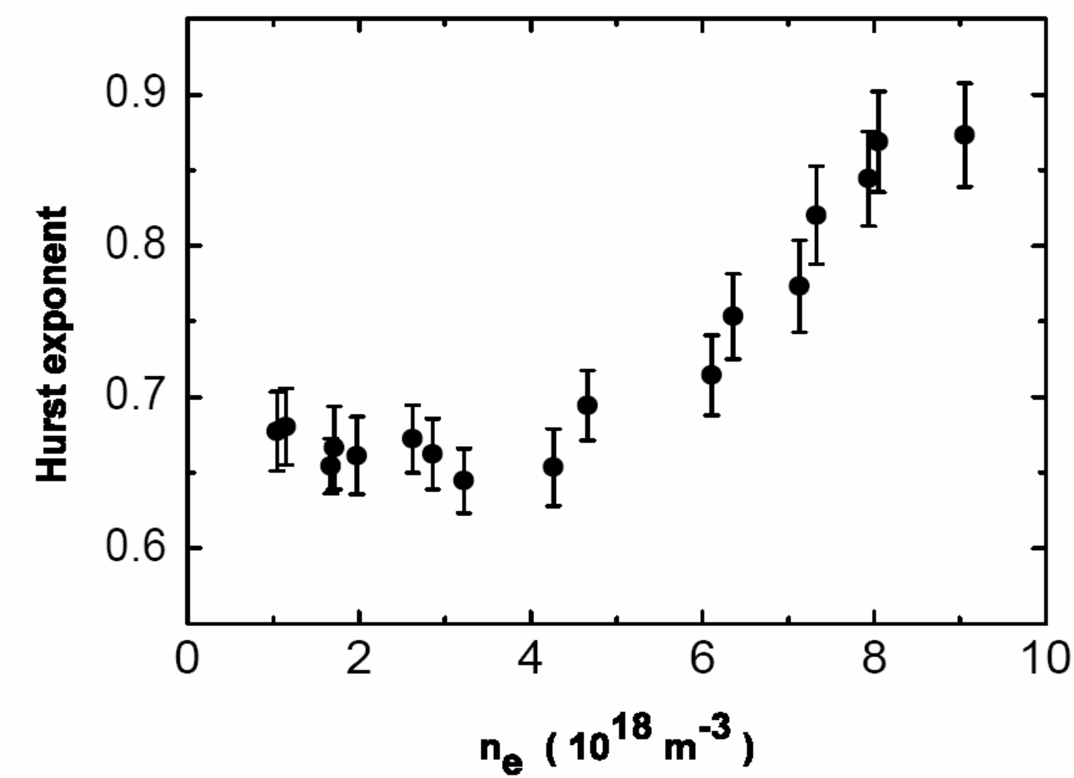

Fig. 9 Profile of the Hurst exponents, *H*, versus the electron density. The Hurst exponent, an indication of the long-range time correlations of the flux time series, is evaluated from the R/S statistics. We can see that at all measured positions the values of *H* are larger than 0.5, i.e. there exist long-range time dependencies in the turbulent transport in SUNIST edge. Furthermore, as the density increases, the values of *H* are greater than 0.8, indicating a stronger long-range time dependencies.

Calculation of the intermittency parameter *C* (1)

Given a time series of the fluxes { $\Gamma_r(i)$, $i = 1, 2, \ldots, N$}, the fluctuations of the $\Gamma_r(i)$ is defined as

$$\widetilde{\Gamma}(i) = \Gamma(i) - <\Gamma(i)> \qquad (1)$$

here and hereafter <...> is time average, the variance of the $\Gamma_r(i)$ is written as $Var\,\Gamma_r$. Introduce a measure

$$\varepsilon(1,i) = \widetilde{\Gamma}_r^2 / Var\ \Gamma_r(1,i) \qquad (2)$$

Then we construct a set of new records by averaging the measure over overlapping subblocks with different time scales, T, from the original flux series $\Gamma_r(t)$. The averaged measure is defined as

$$\varepsilon(T,i) = \frac{1}{T}\sum_{j=0}^{T-1}\varepsilon(1, i+j-m) \qquad (3)$$

Here m is the overlopping number of the two neighbor subblocks. For a self-similar time series, it's q-moment of the measures over the scale T, $<\varepsilon(T, i)^q>$, may have a power law as follow:

$$\left\langle \varepsilon(T,i)^q \right\rangle \approx (T/N)^{-K(q)} \qquad (4)$$

If the series is pure self-similarity case (monofractal behavior), the $K(q)$ scales asymptotically as a linear function of q; But for multifractal case, the $K(q)$ has a nontrivial dependence on q. Knowing the $K(q)$, we can define the intermittency parameter $C(1)$:

$$C(1) = dK(q)/dq\Big|_{q=1} \qquad (5)$$

For our experiment data, we take the $T = 1, 2, \ldots, 200$ μs, then calculate $<\varepsilon(T, i)^q>$ with different q for signals from each radial position.

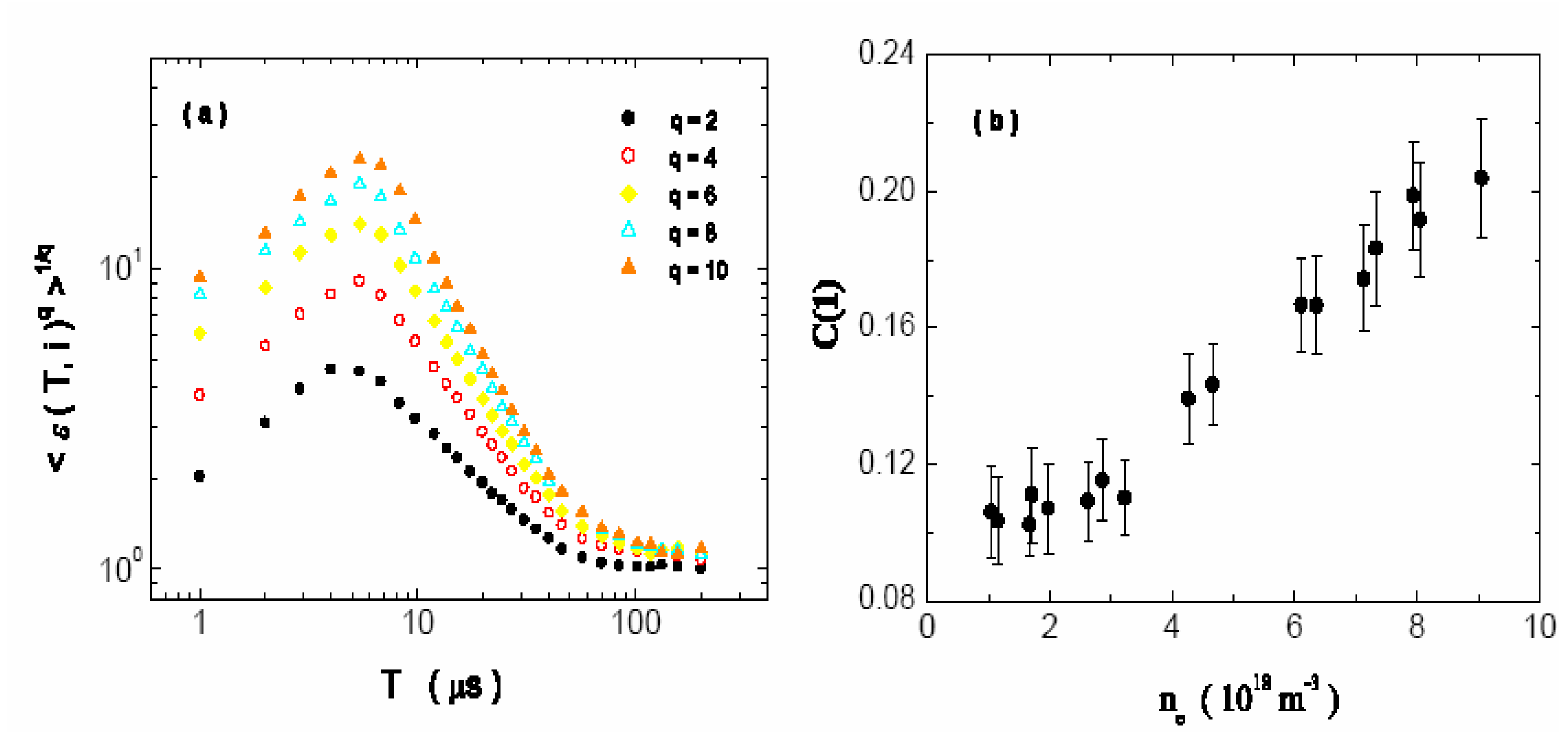

Fig. 10 (a) $1/q$ power of the moments of the flux measure in the fluctuation range of time scales for the data from the radial position r = 52 cm; (b) the profile of the intermittency coefficient of the fluxes as a function of the electron density. In low density region, the values of the $C(1)$ change little within 0.1 ~ 0.12. As the probes radially move inwards and the density increases, the intermittency level corresponds to rise up to 0.2. This result agrees with the bursty feature of the fluctuations of fluxes at high density.

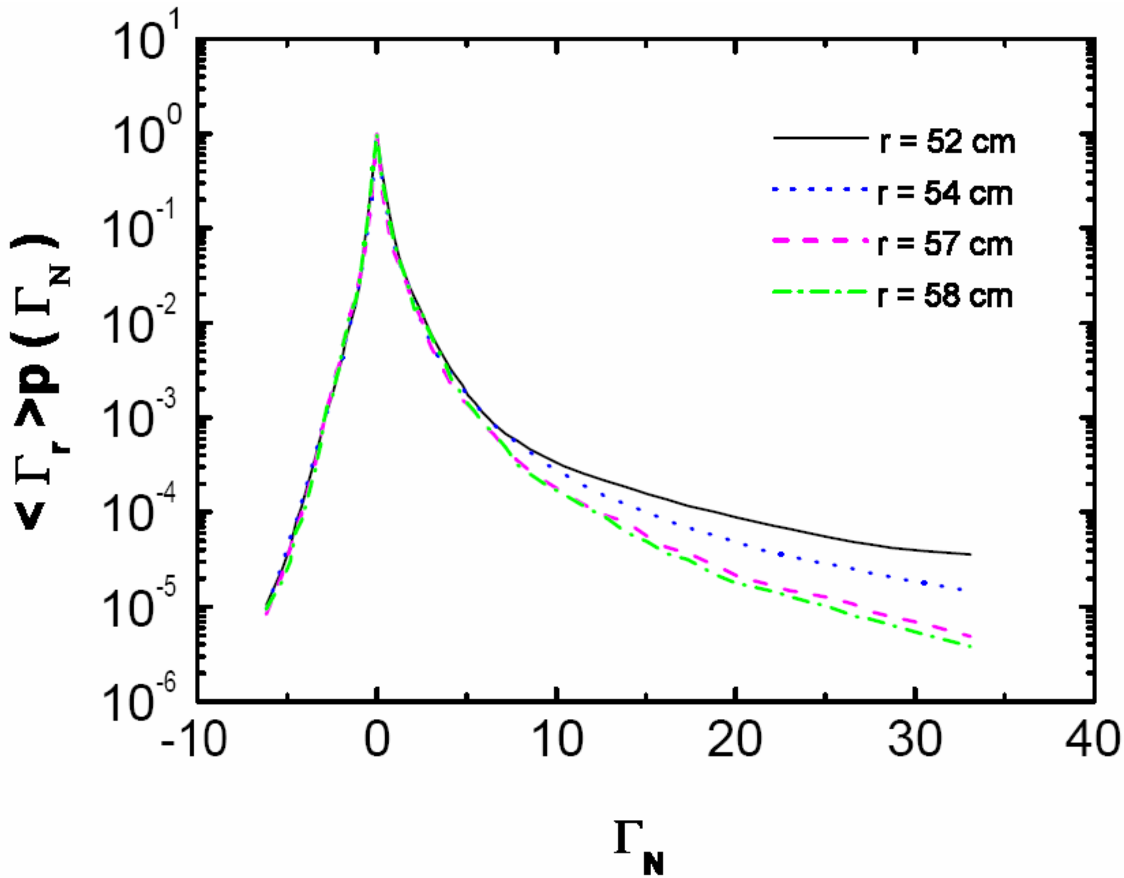

Fig. 11 Comparison of the normalized PDF of the fluxes measured in four different radial positions. We can see that all four PDFs have a clear non-Gaussian long time lag tails, which are the signature of long-range correlation transport events. Furthermore, the PDFs in high-density case (at plasma edge) have a little larger tails than that in low-density case (at SOL).

Summary

1. Distributions of the plasma parameters

- Electron temperature, density, floating potential and plasma potential have radial gradients which supply the free energies for anomalous transports.
- There exits a sheared radial electric field near the limiter radial position.
- The toroidal plasma flow velocity has radial shear at the poloidal velocity shear layer, which may have correlation with the form of the radial electric field.

2. Observation of intermittent transport events

- Edge transport fluxes have intermittency character whose features vary with density.
- The Hurst exponents are greater than 0.5 in all measured radial positions, which means that the transport events have long-range correlation character.
- Distributions of *H* exponents, conditional averaging and PDFs of the particle fluxes show that the infrequent but large transport events are more important in high density than that in the low density.

The End

Thanks All